ACS APPLIED BIO MATERIALS

www.acsabm.org Article

Mechanochemical Drug Conjugation via pH-Responsive Imine Linkage for Polyether Prodrug Micelles

Sohee Han, Joonhee Lee, Eunkyeong Jung, Suebin Park, Aoi Sagawa, Yuji Shibasaki, Dongwon Lee, and Byeong-Su Kim*

Cite This: *ACS Appl. Bio Mater.* 2021, 4, 2465−2474 Read Online

ACCESS | Metrics & More | Article Recommendations | Supporting Information

ABSTRACT: Prodrug-type polymer−drug conjugates based on highly biocompatible functional polyethers are developed through mechanochemical post-polymerization modification. Herein, we design functional epoxide monomers of ethoxyethyl glycidyl ether (EEGE) and azidohexyl glycidyl ether (AHGE) and synthesize diblock copolyethers of PEEGE-*b*-PAHGE via sequential anionic ring-opening polymerization. Subsequent conversion of the functional monomers to the corresponding hydroxyl and amine groups allows for the preparation of double hydrophilic block copolyethers. Most notably, mechanochemical modification allows for the conjugation of these polymers with a highly hydrophobic and potent anticancer agent, cinnamaldehyde, through an imine linkage. The self-assembly of the resulting polymer−drug conjugates into polymeric micelles is characterized by dynamic light scattering and atomic force microscopy. The pH-responsive cleavage of the imine linkages under acidic conditions leads to the release of cinnamaldehyde with a concomitant disassembly of the polymeric micelles. The superior biocompatibility coupled with the solvent-less mechanochemical conjugation approach provides a convenient means to introduce various therapeutics for smart drug delivery.

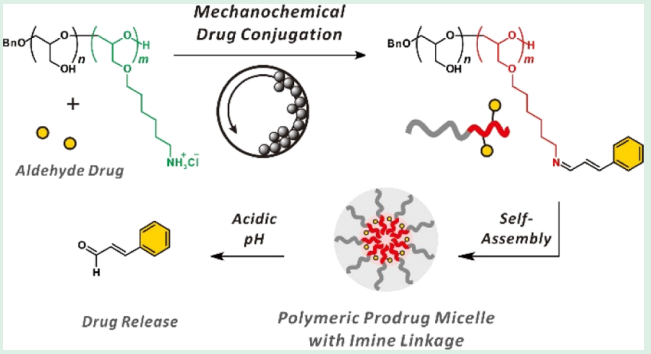

KEYWORDS: *mechanochemistry, polymer−drug conjugates, anionic ring-opening polymerization, post-polymerization modification, imine*

INTRODUCTION

Over the past few decades, drug delivery systems have advanced to achieve time-controlled and site-specific delivery of therapeutic agents to enhance the efficacy of drugs while minimizing undesirable side effects and nonspecific distribution in the body.[1,2] For this reason, self-assembled nanostructures, including liposome, dendrimer, and micelle, have long been exploited as potential drug delivery carriers.[3] While the utilization of these carriers is critical to therapeutic agents with limited aqueous solubility and poor stability, it is still highly desirable to achieve the enhanced loading capacity with tunable release profiles.

In this context, the prodrug-based approach is receiving increasing attention as a promising strategy for the sophisticated delivery of active therapeutics in a controllable manner. Generally, there are three types of prodrug strategies: conjugation of drugs to a pre-synthesized polymer,[4] conjugation of drugs to a monomer prior to polymerization,[5] and growing a polymer chain from a functionalized drug.[2] Specifically, a conjugation-to approach introduces therapeutic agents to a wide spectrum of carriers beyond polymers, such as antibody and peptide.[6,7] Moreover, the linkage between the drug and carrier provides a facile means to control the release of the payload in specific environments.

For that purpose, pH-responsive polymeric systems are particularly appealing to selectively release therapeutics by exploiting the various pH gradients that exist in specific cellular compartments.[8−10] The application of these polymers can further be expanded to other biological applications, including tumor-targeted delivery of drugs, intracellular delivery of nucleic acids or proteins, treatment of inflammatory diseases, and oral administration.[11,12] For example, imines, hydrazides, hydrazones, orthoesters, and acetal linkages degrade selectively in response to pH changes.[13,14] Among them, the imine linkage is of particular interest owing to its sensitivity under different acidic conditions, facilitating its widespread utility as a stimuli-responsive linkage.[15,16] As a notable example, Xu and co-workers conjugated doxorubicin to polymers through imine bond and demonstrated its pH-controlled drug release in acidic environments.[17] In addition, Banerjee and co-workers

Received: November 4, 2020
Accepted: January 27, 2021
Published: February 8, 2021

https://dx.doi.org/10.1021/acsabm.0c01437
ACS Appl. Bio Mater. 2021, 4, 2465−2474

Scheme 1. Schematic Representation of the Prodrug Approach via Mechanochemical Drug Conjugation by pH-Responsive Imine Linkage

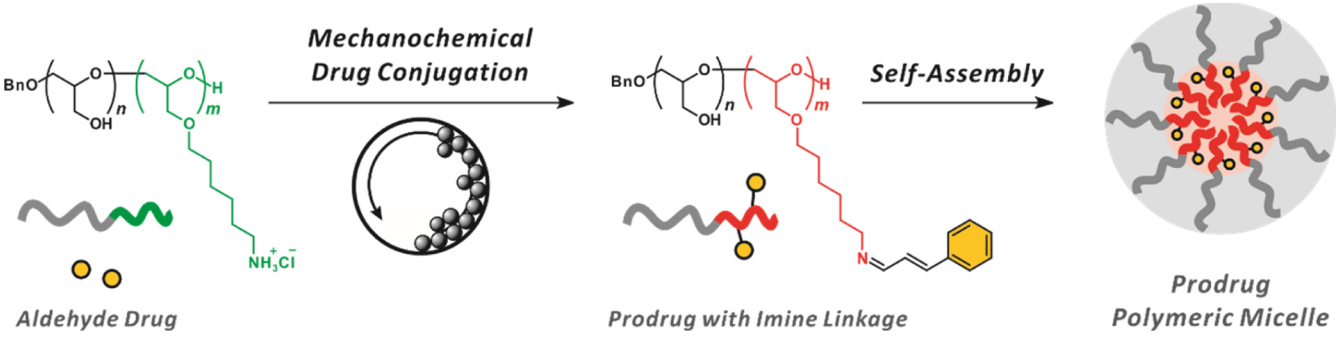

developed pH-responsive glyconanoparticles conjugated to drugs through imine linkages.[18]

Despite active investigations into the prodrug approach with various carriers and therapeutic agents, the difference in solubility between each component can raise significant issues for effective conjugation.[19,20] On the other hand, mechanochemistry offers an alternative means to overcome this solubility limitation by alleviating the need for solvents. Unlike traditional reactions involving solvents, mechanochemistry is performed by mechanical energy, such as grinding and milling, and can be applied to reactants with varying solubilities.[21−23]

Herein, we propose a mechanochemical drug conjugation strategy toward the synthesis of prodrug-type polymer−drug conjugates using highly biocompatible functional polyethers as a platform (Scheme 1). It is well known that the conjugation of poly(ethylene glycol) (PEG) is widely used not only for improving the pharmacokinetics of conjugated therapeutic proteins (i.e., PEGylation)[24,25] but also for facilitating the self-assembly of nanostructures by providing amphiphilic properties to the conjugated hydrophobic therapeutics.[26] Moreover, functional polyethers can provide other advantages, such as various functionalities, that can be synthesized using functional epoxide monomers. Specifically, in this study, novel functional epoxide monomers, such as ethoxyethyl glycidyl ether (EEGE) and azidohexyl glycidyl ether (AHGE), are employed to synthesize diblock copolyethers of PEEGE-*b*-PAHGE via sequential anionic ring-opening polymerization (AROP). Subsequent conversion of the functional monomers to corresponding hydroxyl and amine groups allows for the preparation of double hydrophilic block copolyethers. Moreover, mechanochemical modification allows for the preparation of the prodrug with a potent therapeutic agent, cinnamaldehyde (CA), through an imine linkage. We find that the prepared prodrug can form a self-assembled micellar structure upon mechanochemical conjugation, which in turn exhibits a pH-responsive release of cinnamaldehyde by exploiting the imine linkage. Furthermore, a cell viability assay was performed to evaluate the efficacy of the prodrug toward both normal and tumor cell lines.

EXPERIMENTAL SECTION

Materials. 6-Chloro-1-hexanol, sodium azide, and potassium carbonate (K_2CO_3) were purchased from Alfa Aesar. Tetrabutylammonium hydrogen sulfate ($TBAHSO_4$), epichlorohydrin, ethyl vinyl ether, glycidol, *p*-toluene sulfonic acid monohydrate (*p*-TsOH), phosphazene base *t*-BuP_4 solution (0.8 M in hexane), benzyl alcohol, triphenylphosphine (PPh_3), and cinnamaldehyde were purchased from Sigma-Aldrich and used as received. Toluene and tetrahydrofuran were collected from a solvent purification system and used immediately thereafter. $CDCl_3$ and MeOD were purchased from Cambridge Isotope Laboratories. All chemicals and reagents used were of analytical grade.

Characterizations. ^{1}H NMR spectra were recorded on a Bruker 400 MHz spectrometer at room temperature. The molecular weight (M_n and M_w) and dispersity ($Đ$, M_w/M_n) were determined by gel permeation chromatography (GPC) analysis on an Agilent 1200 series, with THF as the eluent at 25 °C and a flow rate of 1.0 mL min^{-1}, using a refractive index (RI) detector. All calibrations were carried out using poly(methyl methacrylate) (PMMA) and polystyrene standards. FT-IR spectra were recorded on an Agilent Cary 630 FT-IR spectrometer equipped with an ATR module. Differential scanning calorimetry (DSC) (Q200 model, TA Instruments) was carried out under a nitrogen atmosphere in a temperature range of −90−70 °C using a heating rate of 10 °C min^{-1}. Retsch Mixer Mill MM 400 was used for the ball-milling experiments with a 25 mL stainless-steel vessel and 7 mm stainless-steel balls. The critical micelle concentration (CMC) was determined by surface tension measurements on a KYOWA interface measurement analysis system (DM300) using the pendant drop method at 25 °C. Size distribution analysis of the micelles was performed by dynamic light scattering (DLS, ELS-1000ZS, Otsuka Electronics). The morphology of the micelles was determined by an atomic force microscope (Park System, NX-10) via a noncontact mode. The absorbance of the released cinnamaldehyde was analyzed with UV−vis spectroscopy (UV-2550, Shimadzu) and also investigated by high-performance liquid chromatography (HPLC, Shimadzu Prominence).

Synthesis of Glycidyl Ether Monomer. *Synthesis of EEGE.* EEGE was prepared by following a similar method reported previously.[27] Ethyl vinyl ether (28.1 mL, 300.84 mmol) and glycidol (10.0 mL, 150.42 mmol) were dissolved in methylene chloride (150 mL) in a 250 mL round-bottom flask at 0 °C. After the addition, *p*-toluene sulfonic acid monohydrate (286 mg, 1.50 mmol) was slowly added, and the reaction mixture was stirred for 3 h. The reaction mixture was then washed with a saturated $NaHCO_3$ aqueous solution, and the organic layer was separated, dried over Na_2SO_4, and concentrated by rotary evaporation. The product was further purified by distillation under high vacuum and stored over 4 Å molecular sieves. (16.5 g, 112.8 mmol, 75% yield). ^{1}H NMR (400 MHz, $CDCl_3$): δ 4.76 (m, J = 5.4, 3.3 Hz, 1H), 3.90−3.59 (m, 2H), 3.58−3.29 (m, 2H), 3.15 (m, J = 7.3, 3.5, 1.6 Hz, 1H), 2.87−2.74 (m, 1H), 2.62 (m, J = 10.8, 5.0, 2.7 Hz, 1H), 1.40−1.26 (m, 3H), 1.20 (m, J = 7.1, 0.9 Hz, 3H). ^{13}C NMR (101 MHz, $CDCl_3$): δ 99.63, 65.39, 60.86, 50.80, 44.52, 19.65, 15.21.

Synthesis of AHGE. AHGE was prepared following a similar procedure as reported in a previous paper.[28] In a 100 mL round-bottom flask, 6-chloro-1-hexanol (9.90 mL, 74.4 mmol) and sodium azide (7.26 g, 111.6 mmol) were dissolved in water (14.80 mL). Then, the reaction mixture was stirred overnight under reflux. The resulting solution was extracted with ethyl acetate, where the organic phase was washed with brine and dried over Na_2SO_4. The solvent was removed under reduced pressure to yield the intermediate 6-azido-1-

https://dx.doi.org/10.1021/acsabm.0c01437
ACS Appl. Bio Mater. 2021, 4, 2465−2474

Table 1. Characterization of Diblock Copolyethers Synthesized in This Study

no	polymer composition	M_n (PEEGE)/M_n (PAHGE)[a]	$M_{n,NMR}$[b] (g/mol)	$M_{n,GPC}$[c] (g/mol)	$Đ$[c]	T_g[d] (°C)
Az1	$PEEGE_{19}$-*b*-$PAHGE_{17}$	0.82	6200	4500	1.11	−75.8
Az2	$PEEGE_{20}$-*b*-$PAHGE_{10}$	1.47	5000	5000	1.08	−71.1
Az3	$PEEGE_{23}$-*b*-$PAHGE_{5}$	3.38	4500	3300	1.10	−69.7
Az4	$PEEGE_{48}$-*b*-$PAHGE_{9}$	3.91	8900	5400	1.07	−68.2

[a]Ratio of hydrophilic block to hydrophobic block molecular weight. [b]Determined via ^{1}H NMR spectroscopy. [c]Measured using GPC measurements (THF, RI signal, PMMA standard). [d]T_g was determined by DSC at a rate of 10 °C min^{-1}. Please note that the Az polymers are used as precursors for respective Am and Im polymers through post-polymerization modification (see the text for details).

hexanol (9.79 g, 68.4 mmol, 92% yield). Tetrabutylammonium hydrogen sulfate ($TBAHSO_4$) (1.16 g, 3.42 mmol) and epichlorohydrin (30.51 mL, 341.85 mmol) were added to a 40% KOH solution and stirred for 30 min. Then, the intermediate, 6-azido-1-hexanol (9.79 g, 68.4 mmol), was slowly added at 0 °C and the reaction mixture was stirred for 18 h and allowed to reach room temperature. The reaction mixture was subsequently extracted with ethyl acetate, while the organic layer was dried over Na_2SO_4 and concentrated by rotary evaporation. The crude product was purified by column chromatography with a mobile phase of ethyl acetate/hexane (1:5 v/v) to yield AHGE. The product was further purified by distillation under high vacuum and stored over 4 Å molecular sieves (8.04 g, 40.34 mmol, 59% yield). ^{1}H NMR (400 MHz, $CDCl_3$): δ 3.74 (m, J = 11.5, 3.0 Hz, 1H), 3.59−3.44 (m, 2H), 3.39 (m, J = 11.5, 5.8 Hz, 1H), 3.29 (t, J = 6.9 Hz, 2H), 3.17 (m, J = 5.8, 4.1, 2.9 Hz, 1H), 2.82 (dd, J = 5.0, 4.2 Hz, 1H), 2.63 (m, J = 5.0, 2.7 Hz, 1H), 1.62 (m, J = 8.0, 2.6 Hz, 4H), 1.50−1.32 (m, 4H). ^{13}C NMR (75 MHz, $CDCl_3$): δ 71.52, 71.41, 51.40, 50.90, 44.30, 29.55, 28.80, 26.56, 25.70.

Synthesis of PEEGE-*b*-PAHGE Block Copolymers (Az). A mixture of *t*-BuP_4 (0.8 M in hexane, 0.5 mL, 0.48 mmol) and benzyl alcohol (50 μL, 0.48 mmol) in toluene (5 mL) was stirred for 30 min. Each of the glycidyl ether monomers was added in sequence at room temperature. First, EEGE (1.42 g, 9.66 mmol) was slowly added to the solution to initiate the polymerization, while the reaction was monitored by ^{1}H NMR. When the residual epoxide signals of EEGE disappeared, AHGE (0.97 g, 4.83 mmol) was slowly added to the reaction mixture. The reaction was deemed complete when the residual epoxide signals of AHGE disappeared, as determined by ^{1}H NMR. Polymerization was terminated by adding an excess amount of benzoic acid, after which the mixture was passed through a basic alumina pad using THF to remove *t*-BuP_4. The solvent was evaporated to obtain poly(ethoxyethyl glycidyl ether)-*b*-poly(azidohexyl glycidyl ether), $PEEGE_{20}$-*b*-$PAHGE_{10}$ (Table 1, Az2) (1.90 g, 79% yield). ^{1}H NMR (300 MHz, $CDCl_3$): δ 7.32 (m, 5H), 4.69 (m, J = 5.1 Hz, 20H), 4.54 (s, 2H), 3.68−3.40 (m, 210H), 3.27 (t, J = 6.9 Hz, 20H), 1.65−1.54 (m, 40H), 1.42−1.34 (m, 40H), 1.29 (m, J = 5.2 Hz, 60H), 1.19 (m, J = 7.0 Hz, 60H). $Đ$ (GPC, THF, PMMA standard) = 1.08.

Staudinger Reduction of Azide Group and Hydrolysis of Acetal Group (Am). Az2 (1.80 g, 3.6 mmol of azide) was dissolved in THF (20 mL), and the solution was degassed by bubbling N_2 for 20 min. PPh_3 (1.90 g, 7.2 mmol) and water (0.90 mL) were added to the reaction mixture, followed by stirring vigorously at room temperature for 12 h. THF was then evaporated, and 1 M HCl (20 mL) was added. The mixture was subsequently extracted with diethyl ether to remove the remaining triphenylphosphine and triphenylphosphine oxide. The aqueous phase was recovered by lyophilization to yield a viscous polymer (Am2) (1.33 g, 99% yield). ^{1}H NMR (400 MHz, MeOD): δ 7.35 (m, J = 4.5 Hz, 5H), 4.55 (s, 2H), 3.74−3.47 (m, 170H), 2.94 (s, 8H), 1.71−1.55 (m, 40H), 1.43 (m, 40H).

Mechanochemical Conjugation of Cinnamaldehyde (Im). Ball-milling was performed for mechanochemical conjugation. Am2 (44 mg, 0.12 mmol of azide), cinnamaldehyde (45 μL, 0.24 mmol), and K_2CO_3 (34 mg, 0.24 mmol) were added to the vessel, and milling commenced at a frequency of 30 Hz for 30 min. The crude polymer was diluted with methylene chloride, removed inorganic salts by centrifuge, and precipitated into hexane to remove the remained cinnamaldehyde. The cinnamaldehyde-conjugated block copolymer (Im2) was dried under vacuum and employed for further study (46 mg, 86% yield).

Polymeric Micelle Formation and Degradation. A 10.0 mg of sample of the cinnamaldehyde-conjugated block copolymer was dissolved in 0.5 mL of DMF, after which 10.0 mL of water was added dropwise over 1 h using a syringe pump. Then, the mixture was stirred overnight. After dialysis against deionized water for 2 days to exchange the residual DMF, prodrug polymeric micelle dispersions were obtained. The resultant solution was filtered through a syringe filter before DLS and atomic force microscopy (AFM) analysis. The hydrodynamic radius measured by DLS and the line scans measured by AFM were averaged for more than 10 samples. The CMC values of the polymeric prodrug samples were calculated from the crossover point in the plots of surface tension and polymer concentration. To determine the degradation kinetics, the prodrug polymeric micelle solution was placed into a dialysis membrane (MWCO: 3.5 kDa) and incubated in a buffer solution at pH 7.4 and 5.0, prepared using phosphate and acetate buffers, respectively. Samples for the analysis of released cinnamaldehyde by UV−vis spectroscopy and HPLC were taken from the outside of the dialysis membrane.

In Vitro Cell Viability Assay. To evaluate the cellular toxicity of CA-loaded micelles, we carried out a 3-(4,5-dimethylthiazol-2yl)-2,5-diphenyltetrazolium bromide (MTT) assay. SW620 (3×10^5 cells/well) or NIH3T3 cells (2×10^5 cells/well) were treated with various concentrations of CA or CA-loaded micelles and incubated for 24 h. After incubation, cells were treated with 100 μL of an MTT solution (5 mg/mL) and incubated until the formation of formazan crystals. The formazan crystals were dissolved in dimethyl sulfoxide, and the absorbance was detected at a wavelength of 570 nm using a microplate reader (Synergy Mx, BioTek Instrument, Winooski, VT, USA). Cell viability was calculated by comparing the absorbance of untreated cells. To investigate the cellular uptake and endosomal escape, Nile Red-loaded Im2 and Im3 prodrug micelles (50 μg/mL) were treated on SW620 cells (3×10^5 cells/well). After 1 and 24 h of pre-incubation with each sample, cells were treated with LysoTracker for 1 h. A fluorescence image was acquired using a confocal laser scanning microscope (LSM 880, Carl Zeiss, Germany).

RESULTS AND DISCUSSION

Synthesis and Characterization of Functionalized Polyethers. Glycidyl ether monomers can be developed into polyethers, which possess high aqueous solubility and biocompatibility, via AROP. In this regard, two types of functionalized glycidyl ethers, EEGE and AHGE, were initially prepared and polymerized to develop the prodrug carriers. Unlike a conventional PEG block, we choose PEEGE as a hydrophilic block owing to the ease of monomer handling and polymerization. Specifically, EEGE was derived from the reaction between glycidol and ethyl vinyl ether, as reported previously.[29] Moreover, a novel azide-functionalized glycidyl ether, AHGE, was synthesized by a two-step reaction, as recently reported by our group.[28] AHGE is particularly useful as it allows facile chemical modification of the amine groups while maintaining compatibility during AROP. Each monomer was purified by vacuum distillation before polymerization. The

https://dx.doi.org/10.1021/acsabm.0c01437
ACS Appl. Bio Mater. 2021, 4, 2465−2474

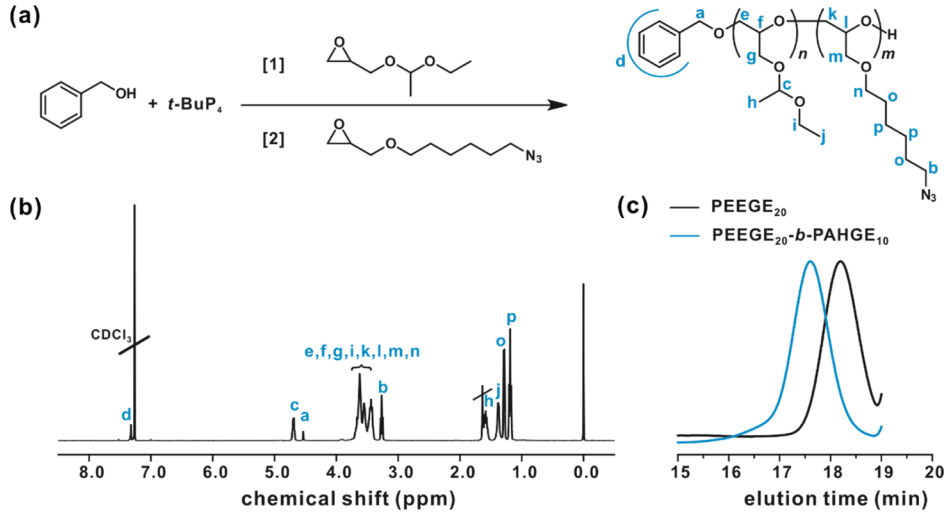

Figure 1. Characterization of synthesized diblock copolyethers. (a) Copolymerization of EEGE and AHGE by AROP with a phosphazene base, (b) ^{1}H NMR spectra of PEEGE$_{20}$-*b*-PAHGE$_{10}$ (Az2 in Table 1), and (c) GPC traces of homopolymer PEEGE$_{20}$ and its diblock copolymer, PEEGE$_{20}$-*b*-PAHGE$_{10}$ (Az2 in Table 1) in THF.

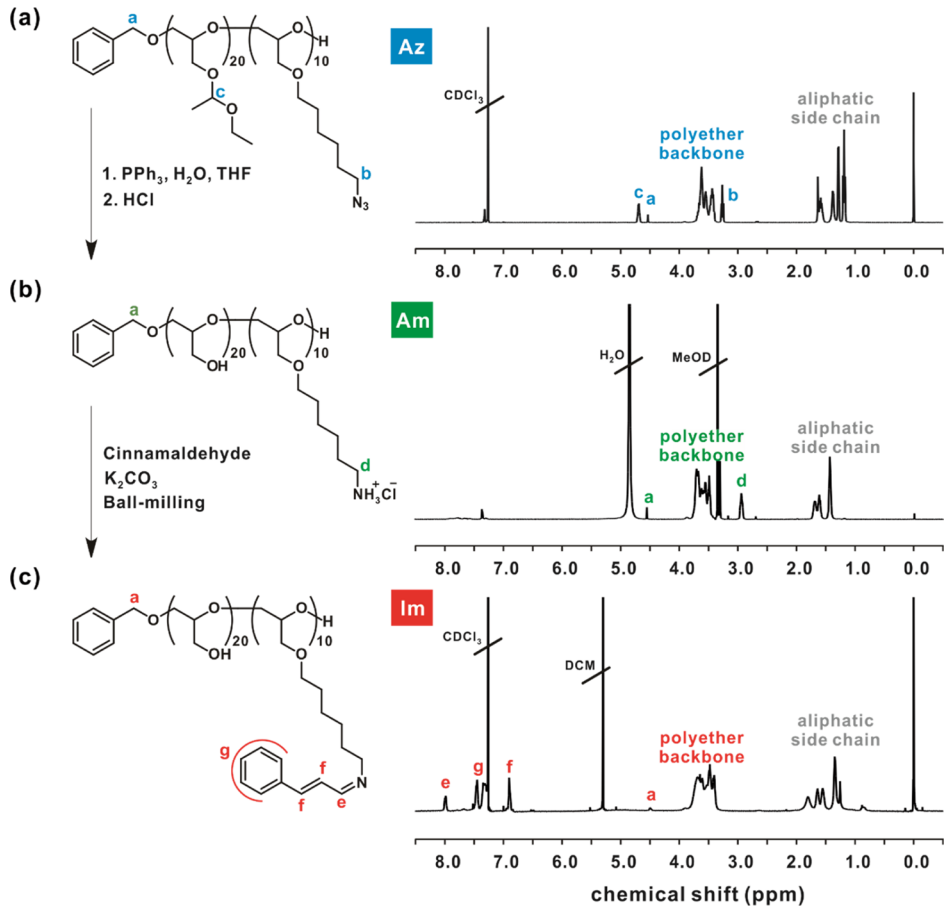

Figure 2. Representative post-polymerization modification procedures with the corresponding ^{1}H NMR spectrum of (a) PEEGE$_{20}$-*b*-PAHGE$_{10}$ (Az2 in Table 1) through (b) Staudinger reduction and hydrolysis (Am2 polymer), and (c) mechanochemical conjugation of cinnamaldehyde (Im2 polymer). (a,c) are measured in $CDCl_3$, whereas (b) is measured in MeOD.

chemical structure of AHGE was successfully confirmed using ^{1}H and ^{13}C NMR spectroscopy (Figures S1−S5).

The copolymerization of EEGE and AHGE was carried out by AROP using benzyl alcohol as an initiator. We introduced an organic superbase, *t*-BuP$_4$, possessing high basicity and low nucleophilicity, in order to control the polymerization of both monomers under mild reaction conditions with a quantitative conversion of EEGE and AHGE of over 99%. The representative ^{1}H NMR spectra of the diblock copolyethers demonstrated the characteristic peaks corresponding to the benzylic proton of the initiator (*a*, 4.55−4.57 ppm), the acetal group of EEGE (*c*, 4.67−4.77 ppm), and the methylene peak

https://dx.doi.org/10.1021/acsabm.0c01437
ACS Appl. Bio Mater. 2021, 4, 2465−2474

adjacent to the azide group of AHGE (*b*, 3.25−3.32 ppm) (Figure 1b). In addition, the complete shift of the GPC trace to a higher molecular weight, with a narrow distribution after subsequent monomer addition, is indicative of well-controlled polymerization systems (Figures 1c and S6). Furthermore, the acetal moiety remained stable under termination by benzoic acid. The residual phosphazene base was found to be completely removed for further biological applications (Figure S7).

The characterizations of a series of diblock copolymers, with different ratios of hydrophilic PEEGE block to hydrophobic PAHGE block molecular weights, are reported in Table 1. The molecular weight ($M_{n,NMR}$) was determined by calculating the ratio of each monomer to initiator using the peak integrals in the ^{1}H NMR spectra. The GPC spectra of all copolyethers showed a narrow dispersity ($Đ$ = 1.01−1.11) (Figure S8). Furthermore, the glass-transition temperature (T_g) of the PEEGE-*b*-PAHGE block copolymers (Az polymers) was revealed to be lower than that of PEG (T_g of −66 °C with M_n = 8000). The observed low T_g values of the prepared Az polymers originated from the flexibility of the linear aliphatic chain substitutions along the backbone (Figure S9).[30]

Mechanochemical Drug Conjugation with Functionalized Polyethers. The pendant azide moieties of Az can be reduced to amines by post-polymerization modification, which offers an alternative to overcome the limitation of direct AROP with primary amine moieties. Specifically, the Staudinger reduction of the azide groups in the PAHGE block occurred with PPh_3 and water followed by additional acidic treatment to remove the acetal groups of the PEEGE block, resulting in the desired amine polymers (Am polymers). The successful post-polymerization modification of the functional groups was confirmed by ^{1}H NMR (Figures 2 and S10).

The presence of ammonium and hydroxyl groups in the side chains of the Am polymers significantly enhanced the polarity. However, it was difficult to isolate the neutralized amine polymers from the aqueous layer due to the increased solubility of the Am polymers in water. This limited solubility prevents the effective conjugation of highly hydrophobic therapeutic agents, which thus prompted us to explore the mechanochemical conjugation approach to overcome this solubility issue. Unlike the typical imine formation conditions, in which molecular sieves or other apparatus are essential in removing the water byproduct, the mechanochemical imine formation is particularly useful. Similarly, Kim and co-workers reported the mechanochemical Schiff base formation using a poly(4-vinylbenzaldehyde) with a series of amine derivatives.[31]

Inspired by this early development, we used a mixture of Am polymers with cinnamaldehyde and potassium carbonate placed in a stainless container with three stainless balls of 7 mm in diameter. Without any additive, the vessel was sealed and placed into a mixer mill at a frequency of 30 Hz for 30 min (see the Experimental section for details). Interestingly, it was found that approximately 100% conversion, based on the comparison between the ^{1}H NMR spectra of the cinnamaldehyde and polymer, was achieved within 30 min, indicating the appearance of protons adjacent to the imine and corresponding to the peak at 7.98−8.04 ppm (Figures 2c and S11).

For further confirmation of the sequential transformation of the polyether side chain functionality, FT-IR analysis was conducted (Figure 3). The prevalent bands in the ranges of 1060−1080 cm^{-1} and 2850−2930 cm^{-1} result from the polyether backbone. The disappearance of the characteristic

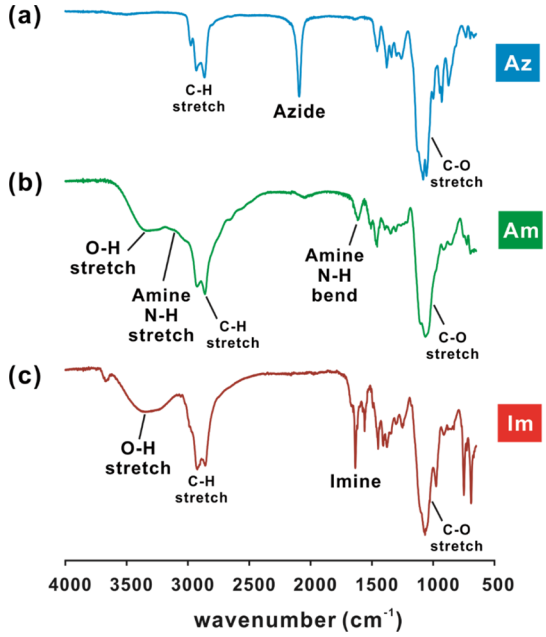

Figure 3. FT-IR spectra of sequential post-polymerization modifications of (a) $PEEGE_{20}$-*b*-$PAHGE_{10}$ (Az2 in Table 1) through (b) Staudinger reduction and hydrolysis (Am2 polymer), and (c) mechanochemical conjugation of cinnamaldehyde (Im2 polymer).

azide peak at 2092 cm^{-1} was observed with the appearance of a broad amine and hydroxy signal at 3650−3100 cm^{-1} after Staudinger reduction and hydrolysis of the acetal group. Moreover, the successful mechanochemical conjugation between cinnamaldehyde and the Am polymer is evidenced by the appearance of the characteristic imine peak at 1636 cm^{-1}.

Independent to this observation, the sequential Staudinger reduction and mechanochemical imine formation were monitored by GPC (Figure S12). While the Az polymer displayed a monomodal peak using RI signal, there was no signal for the Im polymer, possibly due to the similar RIs of both the reference and sample. On the other hand, the mechanochemical conjugation of cinnamaldehyde onto the Am polymers showed a monomodal peak under UV−vis detection as well as a modest molecular weight change that coincided with the theoretical molecular weight changes (Table S1).

Self-Assembly Behavior of Polymeric Prodrug. Owing to the amphiphilic nature of the Im polymers upon mechanochemical conjugation of hydrophobic cinnamaldehyde onto hydrophilic Am polymers, the self-assembly behavior of the resulting micelles was evaluated by measuring the CMC of the Im polymers (i.e., cinnamaldehyde-conjugated prodrugs). Specifically, we used the surface tension method instead of the well-known fluorescence probe method as the latter interfered with the broad absorption of cinnamaldehyde. The relationship between the surface tension of the aqueous solution and the concentration of each Im polymer is illustrated (Figure S13).[32,33] The surface tension of the solution decreased with the increasing polymer concentration, finally reaching a constant value corresponding to the CMC of the respective polymer. In all cases of the cinnamaldehyde-conjugated prodrugs, crossover points were observed, suggesting the successful formation of micelles. Moreover, as the hydrophilicity of Im increased, a higher CMC value was

https://dx.doi.org/10.1021/acsabm.0c01437
ACS Appl. Bio Mater. 2021, 4, 2465−2474

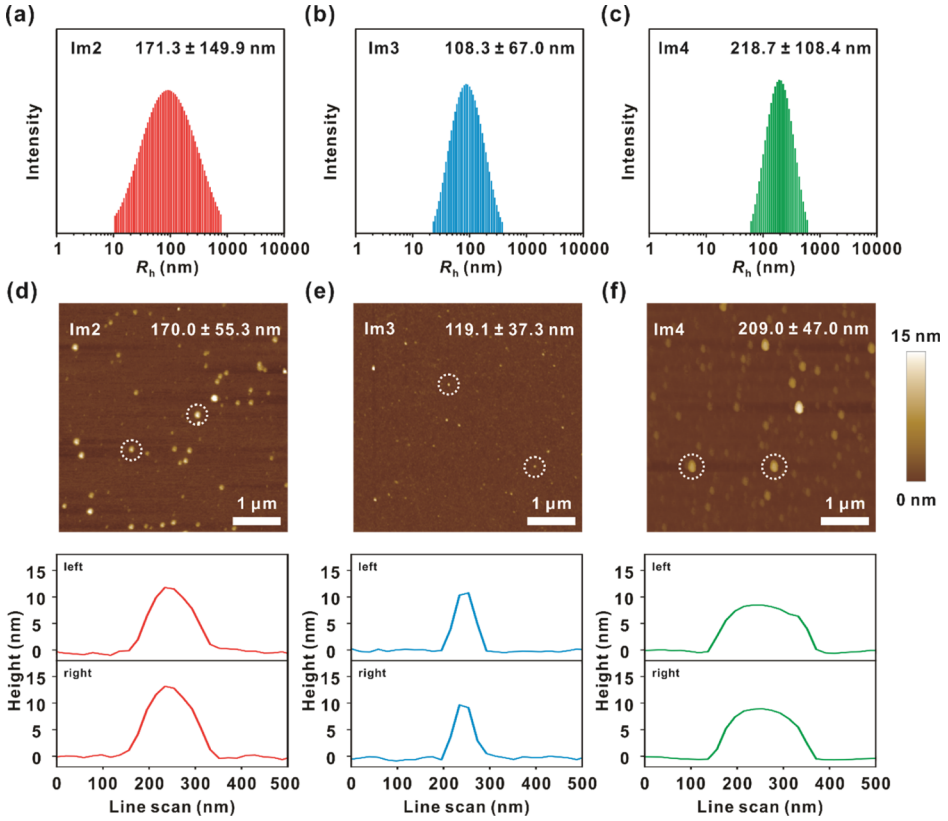

Figure 4. (a–c) Distribution of the hydrodynamic radius (R_h) of the Im micelles in water measured by DLS. (d–f) Representative morphology of Im micelles measured by AFM with corresponding line scan profiles.

measured; 0.735, 0.817, 0.853, and 0.916 mg/mL for Im1, Im2, Im3, and Im4, respectively. It is of note that the CMC value obtained in this study is generally higher than the other block copolymers with similar structures possibly due to the limited solubility of Im polymers upon conjugation with cinnamaldehyde.

After confirming the self-assembly of polymeric prodrugs, the hydrodynamic radius (R_h) of the polymeric micelles was measured by DLS (Figure 4a–c). It was found that the R_h of the polymeric micelles varied depending on the hydrophilic–hydrophobic ratio in the increasing order of Im3, Im2, and Im4. However, it was noted that the Im1 polymer did not show a stable micelle structure under DLS. This could possibly be due to the high hydrophobicity of the Im1 polymer, resulting in the formation of large-sized aggregates with limited dispersity in aqueous media.

It was found that the polymeric micelles derived from Im3 were smaller than those of Im2. This observation suggests that the size of the micelles can be determined by the number of conjugated drugs. For example, the higher loading of cinnamaldehyde into the prodrug micelles of Im2 (prepared from $PEEGE_{20}$-*b*-$PAHGE_{10}$) was twice as much as that of the micelles of Im3 (prepared from $PEEGE_{23}$-*b*-$PAHGE_5$). Furthermore, at a similar hydrophilic/hydrophobic block ratio between Im3 and Im4, it was found that the higher molecular weight of Im4 increased the size of the micelles compared to Im3. Therefore, the polymer composition, particularly both the hydrophilic/hydrophobic block ratio and the overall molecular weight, can control the dimensions of the resulting polymeric micelles. Also, AFM images further demonstrated that these micelles possess a spherical morphology with a particle size in accordance with DLS measurements (Figure 4d–f).

Degradation of Polymeric Prodrug in Acidic Environments. Reversible degradation is critical in carrier-linked type prodrug systems because the prodrugs can only exhibit their therapeutic effect upon release in the active form of the drugs. We first evaluated the degradation of the prodrug micelles by treating them with an aqueous HCl solution and found that the ^{1}H NMR spectrum of the residual polymers matched with that of the Am polymers, indicating successful degradation of the imine linkages and subsequent liberation of the micelles (Figure S14). It is also of note that all micelles degraded into a highly biocompatible double hydrophilic block copolymer that could readily be cleared from the body.

Additionally, to verify the acid-labile cleavage of the prodrug micelles, the release of cinnamaldehyde from the micelles was studied at pH 5.0 and pH 7.4 (Figures 5 and S15–S16). As expected, the prodrug micelles exhibited a pH-responsive release of cinnamaldehyde upon the hydrolysis of the imine linkages. Specifically, the release rates of the prodrug micelles of Im2 at pH 5.0 were clearly higher than those at pH 7.4. For example, the prodrug micelle released 61% of cinnamaldehyde within 24 h and liberated 65% after 4 days at pH 5.0. In contrast, the amount of released cinnamaldehyde was 43% after 24 h at pH 7.4. As suggested in other reports, the accelerated release of cinnamaldehyde under acidic conditions is desirable for effective cancer therapy because the intracellular endosomal pH within the tumor cells is considerably lower than that of normal tissue.[34]

Internalization and Endosomal Escape of Prodrug Micelles. The endocytic pathway is the major cellular uptake

https://dx.doi.org/10.1021/acsabm.0c01437
ACS Appl. Bio Mater. 2021, 4, 2465–2474

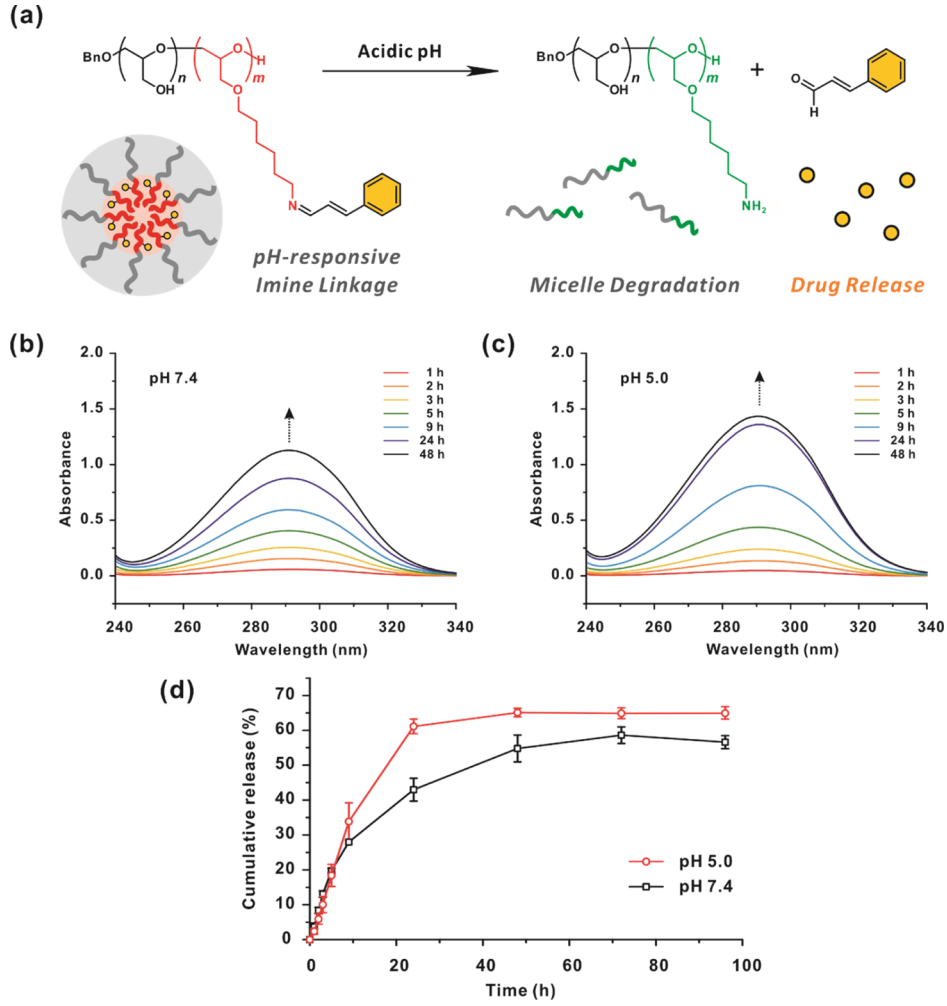

Figure 5. (a) Schematic illustration of polymeric micelle degradation, (b,c) UV−vis spectra, and (d) cumulative release profiles of cinnamaldehyde from prodrug micelles of Im2 under respective pH conditions.

mechanism of biological agents, and these agents become entrapped in endosomes that are fused with lysosomes containing a degrading enzyme, lysozyme. Once taken up by cells, drug delivery systems must overcome the endosomal entrapment and release drug payloads in the cytosol of cells to fully realize therapeutic activity of drugs.[35] Cellular uptake and endosome escape of Im2 and Im3 prodrug micelles were analyzed using confocal fluorescence microscopy (Figures 6 and S17). After pre-incubation with Nile Red-loaded prodrug micelles, SW620 cells were stained with LysoTracker to visualize the acidic lysosomes. After 1 h incubation, yellow fluorescence was observed because of the colocalization of red signal from Nile Red-loaded Im2 and Im3 micelles and green signal from endosomes and lysosomes labeled with LysoTracker, demonstrating the endocytosis and accumulation of prodrug micelles in acidic lysosomes. Eventually, the red fluorescence had spread to cytosol after 24 h incubation with significantly decreased LysoTracker green fluorescence, demonstrating the endosomal escape of Nile Red-loaded Im2 and Im3 prodrug micelles. The endosomal escape could be explained by the influx of protons and osmotic pressure buildup in acidifying endosomes induced by acid-triggered degradation of Im2 and Im3 prodrug micelles.

Anticancer Activity of Polymeric Prodrug. Encouraged by the successful mechanochemical conjugation of the

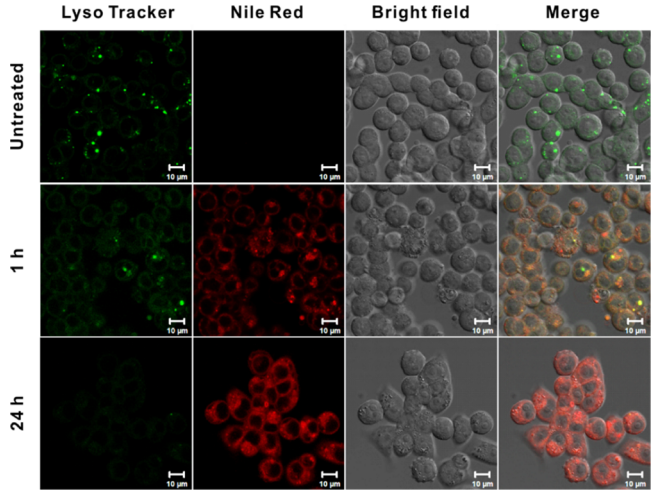

Figure 6. Confocal fluorescence microscopy images of SW620 cells treated with Nile Red-loaded Im2 micelles to evaluate the cellular uptake and endosomal escape of prodrug micelles.

cinnamaldehyde and control over the release kinetics of the therapeutics from the prodrug micelles, we evaluated their cytotoxicity to investigate their potential in smart drug delivery systems. In vitro cytotoxicity of each prodrug micelle was

https://dx.doi.org/10.1021/acsabm.0c01437
ACS Appl. Bio Mater. 2021, 4, 2465−2474

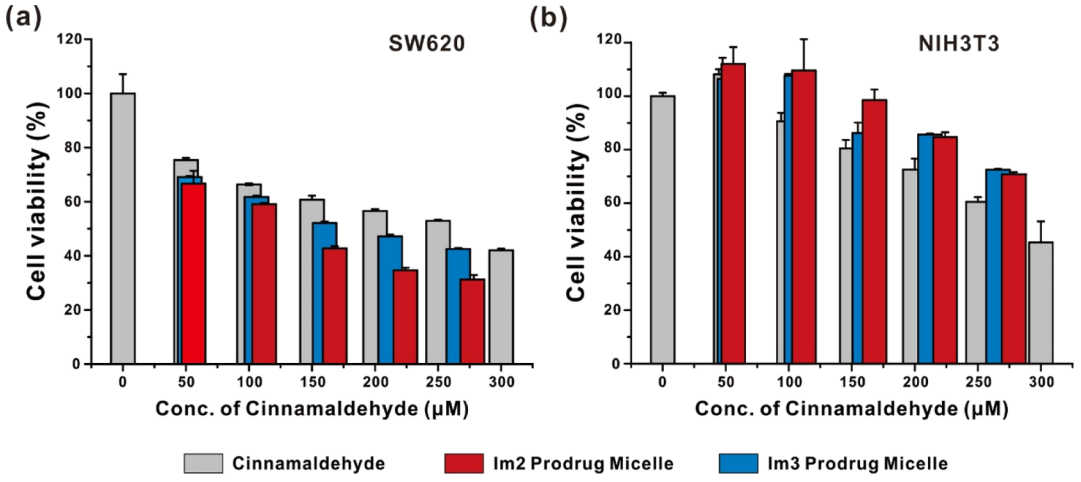

Figure 7. In vitro cell viability assay of Im2 and Im3 prodrug micelles by the MTT assay using (a) SW620 and (b) NIH3T3. Note that the concentration of cinnamaldehyde was used to normalize the differences in the loading contents of the prodrug micelles in reference to free cinnamaldehyde. Data are reported in mean with standard deviation collected from three independent measurements.

assessed via the MTT assay, using cancer cells (e.g., colon cancer cell line SW620) and normal cells (e.g., fibroblast cell line NIH3T3), in comparison to free cinnamaldehyde as a control. As shown in Figure 7, the cinnamaldehyde-loaded prodrug micelles induced considerable cytotoxicity in the SW620 cells, while toxicity was reduced toward the normal NIH3T3 cell lines. The higher cytotoxicity of cinnamaldehyde-loaded prodrug micelles against cancer cells over normal cells can be explained by the notions that cancer cells are under oxidative stress and therefore more vulnerable to oxidative stress-inducing chemotherapeutic agents such as cinnamaldehyde.[36] Moreover, when compared to the free cinnamaldehyde, the cytotoxicity of the prodrug micelles was more effective, thus, ensuring their potential applicability as polymer–drug-conjugated prodrugs. In addition, we determined the cell viability of the carriers themselves as they are released during prodrug degradation. On the basis of an MTT assay, SW620 cells treated with Am2 and Am3 polymer indicated high cellular viability greater than 80%, ensuring its potential as a prodrug carrier (Figure S18).

CONCLUSIONS

In conclusion, cinnamaldehyde-conjugated polymeric micelles were developed as prodrugs loaded with an anticancer agent. A series of PEEGE-*b*-PAHGE block copolymers were synthesized by AROP using two different functional epoxide monomers, EEGE and AHGE. The side chains of the copolyethers were modified through post-polymerization modification to respective hydroxyl and amine functional moieties in the polyethers. Subsequently, by using the ball-milling method, the aldehyde-based anticancer agent, cinnamaldehyde, was mechanochemically conjugated to the polymer through imine linkages. These polymer–drug conjugates were self-assembled into polymeric micelles in aqueous solution and found to undergo controlled degradation in acidic conditions. The biocompatibility and the efficacy of the polymer–drug carriers were evaluated by cell viability assay. The superior biocompatibility coupled with the solvent-less mechanochemical conjugation approach is anticipated to provide a convenient means to introduce various therapeutics for smart drug delivery.

ASSOCIATED CONTENT

Supporting Information

The Supporting Information is available free of charge at https://pubs.acs.org/doi/10.1021/acsabm.0c01437.

Additional ^{1}H and ^{13}C spectrum of the monomers; ^{1}H NMR, GPC, and DSC data of the polymers; surface tension measurements; release profile; and cell viability assay (PDF)

AUTHOR INFORMATION

Corresponding Author

Byeong-Su Kim – *Department of Chemistry, Yonsei University, Seoul 03722, Republic of Korea;* orcid.org/0000-0002-6419-3054; Email: bskim19@yonsei.ac.kr

Authors

Sohee Han – *Department of Chemistry, Yonsei University, Seoul 03722, Republic of Korea;* orcid.org/0000-0001-6691-8904

Joonhee Lee – *Department of Chemistry, Yonsei University, Seoul 03722, Republic of Korea;* orcid.org/0000-0002-6043-6821

Eunkyeong Jung – *Department of Polymer Nano Science and Technology, Chonbuk National University, Jeonju 54896, Republic of Korea;* orcid.org/0000-0002-1164-1028

Suebin Park – *Department of Chemistry, Yonsei University, Seoul 03722, Republic of Korea*

Aoi Sagawa – *Department of Chemistry and Biological Sciences, Faculty of Science and Engineering, Iwate University, Morioka, Iwate 020-8551, Japan*

Yuji Shibasaki – *Department of Chemistry and Biological Sciences, Faculty of Science and Engineering, Iwate University, Morioka, Iwate 020-8551, Japan;* orcid.org/0000-0002-9176-0667

Dongwon Lee – *Department of Polymer Nano Science and Technology, Chonbuk National University, Jeonju 54896, Republic of Korea*

Complete contact information is available at: https://pubs.acs.org/10.1021/acsabm.0c01437

https://dx.doi.org/10.1021/acsabm.0c01437
ACS Appl. Bio Mater. 2021, 4, 2465–2474

Notes

The authors declare no competing financial interest.

■ ACKNOWLEDGMENTS

This work was supported by the Samsung Research Funding & Incubation Center of Samsung Electronics under Project Number SRFC-MA1902-05.

■ REFERENCES

(1) Bildstein, L.; Dubernet, C.; Couvreur, P. Prodrug-Based Intracellular Delivery of Anticancer Agents. *Adv. Drug Deliv. Rev.* **2011**, *63*, 3−23.
(2) Vinciguerra, D.; Denis, S.; Mougin, J.; Jacobs, M.; Guillaneuf, Y.; Mura, S.; Couvreur, P.; Nicolas, J. A Facile Route to Heterotelechelic Polymer Prodrug Nanoparticles for Imaging, Drug Delivery and Combination Therapy. *J. Controlled Release* **2018**, *286*, 425−438.
(3) Doane, T. L.; Burda, C. The Unique Role of Nanoparticles in Nanomedicine: Imaging, Drug Delivery and Therapy. *Chem. Soc. Rev.* **2012**, *41*, 2885−2911.
(4) Yu, Y.; Chen, C.-K.; Law, W.-C.; Weinheimer, E.; Sengupta, S.; Prasad, P. N.; Cheng, C. Polylactide-Graft-Doxorubicin Nanoparticles with Precisely Controlled Drug Loading for pH-Triggered Drug Delivery. *Biomacromolecules* **2014**, *15*, 524−532.
(5) Chytil, P.; Etrych, T.; Kostka, L.; Ulbrich, K. Hydrolytically Degradable Polymer Micelles for Anticancer Drug Delivery to Solid Tumors. *Macromol. Chem. Phys.* **2012**, *213*, 858−867.
(6) Bargh, J. D.; Isidro-Llobet, A.; Parker, J. S.; Spring, D. R. Cleavable Linkers in Antibody-Drug Conjugates. *Chem. Soc. Rev.* **2019**, *48*, 4361−4374.
(7) Chung, S. W.; Lee, B. S.; Choi, J. U.; Kim, S. W.; Kim, I.-S.; Kim, S. Y.; Byun, Y. Optimization of a Stable Linker Involved DEVD Peptide-Doxorubicin Conjugate That Is Activated upon Radiation-Induced Caspase-3-Mediated Apoptosis. *J. Med. Chem.* **2015**, *58*, 6435−6447.
(8) Louage, B.; Van Steenbergen, M. J.; Nuhn, L.; Risseeuw, M. D. P.; Karalic, I.; Winne, J.; Van Calenbergh, S.; Hennink, W. E.; De Geest, B. G. Micellar Paclitaxel-Initiated Raft Polymer Conjugates with Acid-Sensitive Behavior. *ACS Macro Lett.* **2017**, *6*, 272−276.
(9) Lundberg, P.; Lynd, N. A.; Zhang, Y.; Zeng, X.; Krogstad, D. V.; Paffen, T.; Malkoch, M.; Nyström, A. M.; Hawker, C. J. pH-Triggered Self-Assembly of Biocompatible Histamine-Functionalized Triblock Copolymers. *Soft Matter* **2013**, *9*, 82−89.
(10) Shenoi, R. A.; Narayanannair, J. K.; Hamilton, J. L.; Lai, B. F. L.; Horte, S.; Kainthan, R. K.; Varghese, J. P.; Rajeev, K. G.; Manoharan, M.; Kizhakkedathu, J. N. Branched Multifunctional Polyether Polyketals: Variation of Ketal Group Structure Enables Unprecedented Control over Polymer Degradation in Solution and within Cells. *J. Am. Chem. Soc.* **2012**, *134*, 14945−14957.
(11) Li, Y.; Bui, Q. N.; Duy, L. T. M.; Yang, H. Y.; Lee, D. S. One-Step Preparation of pH-Responsive Polymeric Nanogels as Intelligent Drug Delivery Systems for Tumor Therapy. *Biomacromolecules* **2018**, *19*, 2062−2070.
(12) Kim, H.-K.; Thompson, D. H.; Jang, H. S.; Chung, Y. J.; Van Den Bossche, J. pH-Responsive Biodegradable Assemblies Containing Tunable Phenyl-Substituted Vinyl Ethers for Use as Efficient Gene Delivery Vehicles. *ACS Appl. Mater. Interfaces* **2013**, *5*, 5648−5658.
(13) Song, J.; Hwang, E.; Lee, Y.; Palanikumar, L.; Choi, S.-H.; Ryu, J.-H.; Kim, B.-S. Tailorable degradation of pH-responsive all polyether micelles via copolymerisation with varying acetal groups. *Polym. Chem.* **2019**, *10*, 582−592.
(14) Park, H.; Choi, Y.; Jeena, M. T.; Ahn, E.; Choi, Y.; Kang, M. G.; Lee, C. G.; Kwon, T. H.; Rhee, H. W.; Ryu, J. H.; Kim, B.-S. Reduction-Triggered Self-Cross-Linked Hyperbranched Polyglycerol Nanogels for Intracellular Delivery of Drugs and Proteins. *Macromol. Biosci.* **2018**, *18*, 1700356.
(15) Xu, X.; Flores, J. D.; McCormick, C. L. Reversible Imine Shell Cross-Linked Micelles from Aqueous RAFT-Synthesized Thermoresponsive Triblock Copolymers as Potential Nanocarriers for "pH-Triggered" Drug Release. *Macromolecules* **2011**, *44*, 1327−1334.
(16) Popescu, M.-T.; Liontos, G.; Avgeropoulos, A.; Voulgari, E.; Avgoustakis, K.; Tsitsilianis, C. Injectable Hydrogel: Amplifying the pH Sensitivity of a Triblock Copolypeptide by Conjugating the N-Termini via Dynamic Covalent Bonding. *ACS Appl. Mater. Interfaces* **2016**, *8*, 17539−17548.
(17) Tao, Y.; Liu, S.; Zhang, Y.; Chi, Z.; Xu, J. A pH-Responsive Polymer Based on Dynamic Imine Bonds as a Drug Delivery Material with Pseudo Target Release Behavior. *Polym. Chem.* **2018**, *9*, 878−884.
(18) Balakrishnan, B.; Subramanian, S.; Mallia, M. B.; Repaka, K.; Kaur, S.; Chandan, R.; Bhardwaj, P.; Dash, A.; Banerjee, R. Multifunctional Core-Shell Glyconanoparticles for Galectin-3-Targeted, Trigger-Responsive Combination Chemotherapy. *Biomacromolecules* **2020**, *21*, 2645−2660.
(19) Kalepu, S.; Nekkanti, V. Insoluble Drug Delivery Strategies: Review of Recent Advances and Business Prospects. *Acta Pharm. Sin. B* **2015**, *5*, 442−453.
(20) Mitragotri, S.; Burke, P. A.; Langer, R. Overcoming the Challenges in Administering Biopharmaceuticals: Formulation and Delivery Strategies. *Nat. Rev. Drug Discovery* **2014**, *13*, 655−672.
(21) Grätz, S.; Beyer, D.; Tkachova, V.; Hellmann, S.; Berger, R.; Feng, X.; Borchardt, L. The mechanochemical Scholl reaction - a solvent-free and versatile graphitization tool. *Chem. Commun.* **2018**, *54*, 5307−5310.
(22) Friščić, T. Supramolecular Concepts and New Techniques in Mechanochemistry: Cocrystals, Cages, Rotaxanes, Open Metal−Organic Frameworks. *Chem. Soc. Rev.* **2012**, *41*, 3493−3510.
(23) Tan, D.; García, F. Main Group Mechanochemistry: From Curiosity to Established Protocols. *Chem. Soc. Rev.* **2019**, *48*, 2274−2292.
(24) Joralemon, M. J.; McRae, S.; Emrick, T. PEGylated Polymers for Medicine: From Conjugation to Self-Assembled Systems. *Chem. Commun.* **2010**, *46*, 1377−1393.
(25) Pelegri-Oday, E. M.; Lin, E. W.; Maynard, H. D. Therapeutic Protein-Polymer Conjugates: Advancing beyond Pegylation. *J. Am. Chem. Soc.* **2014**, *136*, 14323−14332.
(26) Paik, B. A.; Mane, S. R.; Jia, X.; Kiick, K. L. Responsive Hybrid (Poly)Peptide-Polymer Conjugates. *J. Mater. Chem. B* **2017**, *5*, 8274−8288.
(27) Lee, S.; Saito, K.; Lee, H.-R.; Lee, M. J.; Shibasaki, Y.; Oishi, Y.; Kim, B.-S. Hyperbranched Double Hydrophilic Block Copolymer Micelles of Poly(Ethylene Oxide) and Polyglycerol for pH-Responsive Drug Delivery. *Biomacromolecules* **2012**, *13*, 1190−1196.
(28) Lee, J.; Han, S.; Kim, M.; Kim, B.-S. Anionic Polymerization of Azidoalkyl Glycidyl Ethers and Post-Polymerization Modification. *Macromolecules* **2020**, *53*, 355−366.
(29) Taton, D.; Le Borgne, A.; Sepulchre, M.; Spassky, N. Synthesis of Chiral and Racemic Functional Polymers from Glycidol and Thioglycidol. *Macromol. Chem. Phys.* **1994**, *195*, 139−148.
(30) Chieng, B. W.; Ibrahim, N. A.; Yunus, W. M. Z. W.; Hussein, M. Z. Plasticized Poly(Lactic Acid) with Low Molecular Weight Poly(Ethylene Glycol): Mechanical, Thermal, and Morphology Properties. *J. Appl. Polym. Sci.* **2013**, *130*, 4576−4580.
(31) Ohn, N.; Kim, J. G. Mechanochemical Post-Polymerization Modification: Solvent-Free Solid-State Synthesis of Functional Polymers. *ACS Macro Lett.* **2018**, *7*, 561−565.
(32) Rusanov, A. I. The Mass Action Law Theory of Micellar Solutions. *Adv. Colloid Interface Sci.* **1993**, *45*, 1−78.
(33) Stauffer, C. E. The Measurement of Surface Tension by the Pendant Drop Technique. *J. Phys. Chem.* **1965**, *69*, 1933−1938.
(34) Wike-Hooley, J. L.; Haveman, J.; Reinhold, H. S. The Relevance of Tumour pH to the Treatment of Malignant Disease. *Radiother. Oncol.* **1984**, *2*, 343−366.
(35) Reinhold, D. J.; Kondow-Mcconaghy, H. M.; Hager, E. C.; Pellois, J.-P. Endosomal Escape and Cytosolic Penetration of Macromolecules Mediated by Synthetic Delivery Agents. *Bioconjugate Chem.* **2019**, *30*, 293−304.

https://dx.doi.org/10.1021/acsabm.0c01437
ACS Appl. Bio Mater. 2021, 4, 2465−2474

(36) Noh, J.; Kwon, B.; Han, E.; Park, M.; Yang, W.; Cho, W.; Yoo, W.; Khang, G.; Lee, D. Amplification of Oxidative Stress by a Dual Stimuli-Responsive Hybrid Drug Enhances Cancer Cell Death. *Nat. Commun.* **2015**, *6*, 6907.

https://dx.doi.org/10.1021/acsabm.0c01437
ACS Appl. Bio Mater. 2021, 4, 2465−2474